TELLUS

Analysis of anthropogenic CO_2 signal in ICARTT using a regional chemical transport model and observed tracers

By J. E. CAMPBELL[1]*, G. R. CARMICHAEL[1], Y. TANG[1], T. CHAI[1], S. A. VAY[2], Y.-H. CHOI[2], G. W. SACHSE[2], H. B. SINGH[3], J. L. SCHNOOR[1], J. WOO[4], J. M. VUKOVICH[5], D. G. STREETS[6], L. G. HUEY[7] and C. O. STANIER[1], [1]*Center for Global and Regional Environmental Research, University of Iowa, Iowa City, IA 52242, USA;* [2]*NASA Langley Research Center, Hampton, VA 23681, USA;* [3]*NASA Ames Research Center, Moffett Field, CA 94035, USA;* [4]*Northeast States for Coordinated Air Use Management, Boston, MA, 02114 USA;* [5]*Carolina Environmental Program (CEP), University of North Carolina, Chapel Hill, NC, 27599, USA;* [6]*Decision & Information Science Division, Argonne National Laboratory, Argonne, IL, 60439, USA;* [7]*School of Earth and Atmospheric Sciences, Georgia Institute of Technology, Atlanta, GA, 30332, USA*

ABSTRACT

Atmospheric CO_2 inversion studies infer surface sources and sinks from observations and models. These studies usually require determination of the fossil fuel component of the observation, which can be estimated using anthropogenic tracers such as CO. The objective of this study is to demonstrate a new CO tracer method that accounts for overlapping forest fire and photochemical CO influences, and to quantify several aspects of the uncertainty in the CO tracer technique. Photochemistry model results and observations from the International Consortium for Atmospheric Research on Transport and Transformation experiment are used to quantify changes in the fossil fuel CO_2 prediction from the CO tracer method with and without the inclusion of CO from biomass burning and photochemistry. Although the chemical sources and sinks tend to offset each other, there are regions where the chemical reactions change fossil fuel CO_2 predictions by up to ±4 ppm. Including biomass burning lowers fossil fuel CO_2 by an average of 12 ppm in plumes heavily influenced by long-range transport of forest fire CO. An alternate fossil fuel CO_2 calculation is done in a power plant plume using SO_2 as a tracer, giving a change in 20 ppm from the CO method, indicative of uncertainty in the assumed $CO:CO_2$ ratio.

1. Introduction

In order to better predict future climate change and manage carbon emissions, it is essential to understand the processes governing exchanges of carbon between the atmosphere, terrestrial biosphere and oceans. Top-down studies which infer CO_2 surface fluxes from observations of atmospheric CO_2 concentration, provide strong evidence of a net sink of atmospheric CO_2 in the Northern Hemisphere terrestrial environments (Tans et al., 1990; Enting et al., 1995; Fan et al., 1998; Bousquet et al., 2000; Gurney et al., 2002; Gurney et al., 2003; Gurney et al., 2004).

An important step in many top-down experiments is to apportion each CO_2 observation into source/sink components as

follows,

$$^{obs}CO_2 = {}^{ff}CO_2 + {}^{oc}CO_2 + {}^{bio}CO_2 + {}^{bg}CO_2 + {}^{r}CO_2. \quad (1)$$

Here $^{obs}CO_2$ is the observed CO_2 concentration, $^{ff}CO_2$ is the contribution to the observed concentration due to fossil fuel emissions, $^{oc}CO_2$ is the contribution from the ocean surface flux, $^{bio}CO_2$ is the contribution from the seasonally varying, annually balanced biosphere flux, $^{bg}CO_2$ is the background contribution and $^{r}CO_2$ is the residual concentration from less well-known sources and sinks such as deforestation, forest fires, biomass energy emissions and interannual climate variability. The first three terms on the right-hand side of eq. (1) are considered to be relatively well known and are determined by running atmospheric transport models that are driven by surface flux estimates. The $^{r}CO_2$ term is the unknown that is inverted to obtain estimates of residual surface fluxes.

Estimates of the fossil fuel component, $^{ff}CO_2$, are typically obtained by driving atmospheric transport models with fossil

*Corresponding author.

e-mail: cae@engineering.uiowa.edu

fuel emission inventories. The widely used fossil fuel emission inventories have an annual, $1° × 1°$ resolution and are based on statistics of energy consumption, emission factors and population density (Andres et al., 1996; Olivier et al., 1996; Brenkert, 1998).

This CO_2 emissions inventory resolution may be appropriate for inversions of annual fluxes at global scales. However, the emissions resolution could cause large biases for regional scale carbon inversion. Regional scale inversions have spatial resolution of $10^2–10^6$ km^2 and subannual temporal resolution. The seasonal variation of U.S. fossil fuel emissions has an amplitude of 30% (Blasing et al., 2003) and diurnal variation is likely caused by lighting, heating and industrial energy consumption. Side by side comparisons of monthly inversions driven by an annual scale fossil fuel inventory and a hypothetical seasonal-varying inventory resulted in retrieved fluxes that had up to 50% differences (Gurney et al., 2005). In addition to the error due to resolution, there are absolute errors in the inventories that must be considered in regional inversions (Levin et al., 2003).

In order to address the need for improved $^{ff}CO_2$ estimates, the use of observed anthropogenic tracers has been proposed (Wofsy and Harris, 2002). The development of such methods to apply tracers to predict $^{ff}CO_2$ could allow for more accurate top-down studies. This approach could also provide a means for validating fossil fuel emission inventories and carbon trading agreements.

Studies of the effectiveness of using observations of anthropogenic tracers to estimate $^{ff}CO_2$ indicate promise as well as concerns. Measurement of radiocarbon ($^{14}CO_2$) provide the most accurate estimates of $^{ff}CO_2$ but are currently sparse due to complexity and cost, and not yet possible at an hourly resolution (Levin et al., 1989; Zondervan and Meijer, 1996; Turnbull et al., 2006). Sulphur hexafluoride, SF$_6$, which is emitted at industrial sources and electric power stations has been shown to yield large errors in $^{ff}CO_2$ (Turnbull et al., 2006), and thus is a poor choice for this approach.

This paper focuses on the use of CO as an anthropogenic tracer for two reasons: (1) CO is widely measured at high time resolution and (2) the CO tracer approach has been used to estimate $^{ff}CO_2$ in several top-down studies. The CO approach has been applied as,

$$^{ff}CO_2 = (^{obs}CO - {}^{bg}CO)/R. \qquad (2)$$

Here ^{obs}CO is the observed CO concentration, ^{bg}CO is the background CO concentration and R is a ratio relating the CO offset to $^{ff}CO_2$.

Previous work applied the CO approach to hourly tower observations at 30 m, in Harvard Forest (Potosnak et al., 1999). A linear model was fit to the data leading to R values of 12.5–14.2 moles CO/1000 moles CO_2 in winter and 20–28 mol CO/1000 mol CO_2 in the summer, with $^{ff}CO_2$ of 4–5 ppm in winter and 2–3 ppm in summer. Other studies have assumed a fixed ratio, R, of 20 mol CO/1000 mol CO_2, based on ratios from

Potosnak et al. (1999) and ratios from total annual U.S. emissions (Bakwin et al., 1998; Bakwin et al., 2004). More recently, the CO approach has been applied by estimating R and ^{bg}CO, and reactive chemistry using atmospheric transport models driven by emission inventories of CO and CO_2 (Gerbig et al., 2003; Lin et al., 2004).

The major classes of potential error in the CO tracer method include: (1) errors in R; and (2) neglecting the non-anthropogenic sources and sinks of CO that influence the CO observation such as forest fires, partial oxidation of VOC's and the reaction of OH and CO. Gerbig et al. (2003) accounted for non-anthropogenic CO for the COBRA campaign with a simple approach based on climatological values of OH and an assumption that forest fire and fossil fuel components were spatially separated. These results indicate that omitting OH oxidation would yield biased results. We extend this analysis by taking advantage of observed tracers and advanced photochemistry models to estimate the non-anthropogenic CO influences for CO observation where the forest fire and chemical influences are collocated. Sensitivity of $^{ff}CO_2$ to the ratio R is reported by comparing several different methods for calculating R. It should be noted that this work does not comprehensively consider the uncertainty in R as a result of potentially large errors in source inventories, transport, chemistry and the different disaggregation methods for CO and CO_2 inventories. The comprehensive study of the inventory ratios of CO:CO_2 requires either a bottom up study of the errors in the inventories, or a top-down method using the $^{14}CO_2$ method (Turnbull et al., 2006).

The objective of our study is to estimate several of the more significant components of uncertainty in the CO tracer method due to forest fires and photochemistry contributions to the CO observations. These uncertainty components may be used to help explain absolute errors in the CO method found from comparison of CO and $^{14}CO_2$-based estimates of $^{ff}CO_2$. We present a revised CO method that may better account for these contributions to CO and a limited comparison of our CO method uncertainty estimates with absolute error estimates from a study of $^{14}CO_2$ by the NOAA Global Monitoring Division (GMD; Turnbull et al., 2006).s

Atmospheric trace gas observations were taken from the International Consortium for Atmospheric Research on Transport and Transformation (ICARTT) field experiment conducted in the summer of 2004 over North America. The ICARTT observations are an ideal data set for our application for two reasons: (1) the data set includes tracers of many surface fluxes and (2) the observations cover portions of North America where future CO_2 tower observatories are planned. The STEM-2K3 regional air quality model and its adjoint (Carmichael et al., 2003; Tang et al., 2004; Sandu et al., 2005) are applied with the SAPRC-99 chemical mechanism (94 species, 235 chemical reactions, 30 photolytic reactions). Much of the observed and modelled data presented in this study are available online (http://www-air.larc.nasa.gov/missions/intexna/dataaccess.htm).

2. Methodology

2.1. Regional air quality model and emissions

The STEM-2K3 regional air quality model and its adjoint are used in this work. The model employs the SAPRC99 chemical mechanism (Carter, 2000), the SCAPE II aerosol thermodynamics module and an online photolysis solver (Tang et al., 2003). The photolysis reactions are particularly important to CO concentrations because photolysis is the main natural source of the OH radical. The OH radical is the primary oxidizing agent for CO and other reduced carbon trace gases that are oxidized to CO. The contribution to CO$_2$ from the oxidation of hydrocarbons is currently not accounted for in the analysis.

An adjoint model to STEM-2K3 has been developed for sensitivity studies and optimal estimation of model parameters such as emissions and initial conditions (Daescu and Carmichael, 2003; Hakami et al., 2005; Sandu et al., 2005; Chai et al., 2006). We implemented the adjoint analysis to obtain quantitative estimates of the influence regions for observation points along the ICARTT flight paths. A perturbation of the concentration at the observation location, the receptor, is propagated backward in time to determine the sensitivities of the target with respect to the concentrations in each grid cell at previous time steps. The resulting sensitivity value is,

$$\varphi(x, y, z, t) = \frac{\partial CO_2^{receptor}}{\partial CO_2^{x,y,z,t}}. \tag{3}$$

The time-averaged, column maximum values of the adjoint forcing term, ϕ, are computed to provide a map of the influence region as in Sandu et al. (2005).

The input meteorology fields are from the NCAR/PSU MM5 mesoscale meteorological model, driven by NCEP FNL (Final Global Data Assimilation System) $1° \times 1°$ analysed data. Grid nudging was performed every 6 hr, and re-initialization with FNL data took place every 72 hr. The cloud scheme of Grell et al. (1994) was chosen for the physical parametrization, and the MRF scheme (Hong and Pan, 1996) was employed for PBL paramterization. The MM5 simulation was run on a 60 km Lambert Conformal North American domain (Fig. 4). The 21 sigma layers extend from the surface to 100 hPa.

The time-varying boundary conditions for CO$_2$ tracers of the biosphere, ocean and fossil fuel fluxes are provided by the TM5 global chemical transport model (Peters et al., 2004). The TM5 runs are on a $6° \times 4°$ grid and are driven by ECMWF meteorological fields and emissions from the TransCom Continuous Experiment (Law et al., 2005). Boundary conditions for CO, O$_3$ and other trace gases are provided by the MOZART-NCAR global transport model with a 2.8° horizontal resolution and MOPITT-satellite-derived forest fire emissions (Pfister et al., 2005). Model results for CO$_2$ are in units of ppm-molar.

Within the model domain, surface fluxes for CO$_2$ are from the TransCom Continuous Experiment including 1° hourly biogenic fluxes from the Simple Biosphere Model for 2003 (Baker et al., 2003), 1° monthly ocean fluxes for 2000 (Takahashi et al., 1999) and 1° annual fossil fuel emissions for 1995 (Brenkert, 1998). We scaled the fossil fuel emission to 2004 using a least squares fit to U.S. annual emissions data from 1997 to 2003 (Blasing et al., 2004). We scaled the annual 2004 fossil fuel emissions to summer emissions based on the U.S. annual cycle with an amplitude of 30% (Blasing et al., 2003). The interannual factor (1.15) and seasonal factor (0.86) approximately offset each other.

Anthropogenic emissions of CO, O$_3$, SO$_2$, NH$_3$, NO$_x$ and reduced carbon species (VOC's) are from the U.S. EPA National Emission Inventory (NEI) for 2001. These gridded, 4 km, hourly emissions include mobile, point, area and non-road mobile sources. Reporting CO$_2$ emissions is voluntary in the U.S., and the EPA NEI does not include CO$_2$. Biogenic emissions of VOC's were estimated by driving the Biogenic Emission Inventory System 2 (Geron et al., 1994) with the meteorological output from our MM5 runs. The effects of the different scales for these emissions are minimized by averaging to our 60 km model grid. However the possibility of introducing error in the CO:CO$_2$ emission ratio exists due to the interpolation of the CO$_2$ emissions onto the 60 km grid.

Local large point source (LPS) emissions data were obtained from the U.S. EPA Clean Air Markets program (http://cfpub.epa.gov/gdm/). The emissions data included hourly, facility level emissions for 2004.

2.2. ICARTT observations

We used observations of CO$_2$, CO and other trace gases taken from the NASA DC-8 during the ICARTT field campaign in the summer of 2004. Measurements of atmospheric CO$_2$ (± 0.25 ppm-molar uncertainty) and CO ($\pm 2\%$ uncertainty) were obtained with a modified Li-Cor model 6252 non-dispersive infrared analyser and the differential absorption of CO measurement (DACOM) instrument (Sachse et al., 1987), respectively. In-flight calibrations of CO$_2$ were performed every 15 min with standards traceable to the WMO Central Laboratory at NOAA GMD (Vay et al., 2003). Additional grab samples of CO were analysed at U.C. Irvine using a gas chromatograph (HP 5890) equipped with a flame ionization detector and a 3 m molecular sieve column (Barletta et al., 2002). These CO measurements were calibrated using working standards (run every four samples) and using a gravimetrically prepared CO standard from NIST.

A comprehensive set of complementary trace gas measurements was also collected during ICARTT. We focus on acetonitrile data (CH$_3$CN, $\pm 20\%$ uncertainty) as a tracer of forest fires (Lobert et al., 1991) and SO$_2$ as an LPS tracer. Acetonitrile observations were taken with a modified gas chromatographic instrument that had previously been used to measure PAN and oxygenated organics (Singh et al., 2003). SO$_2$ was measured by

chemical ionization mass spectrometry ($\pm 9\%$ uncertainty; Huey et al., 2004).

We analysed observations of $^{14}CO_2$ (± 1.6–2.6% uncertainty), CO_2 and CO made during the summer of 2004 in New England by NOAA GMD (Turnbull et al., 2006). These measurements were taken in the boundary layer and free troposphere at locations in Harvard Forest, Massachusetts ($42°32'$N, $72°10'$W) and Portsmouth, New Hampshire ($42°57'$N, $72°37'$W). Details of the extraction and accelerator mass spectrometry methods are in Turnbull et al. (2006).

2.3. CO tracer methodology

In this study, we employed 4 variations of the CO tracer method to estimate $^{ff}CO_2$ at observation points along the ICARTT flight paths. The first two approaches are the static methods (Bakwin et al., 1998; Bakwin et al., 2004) that use a constant R value of 20. The basic static method is formulated as,

$$^{ff}CO_2 = (^{obs}CO - ^{obs.bg}CO)/20, \tag{4}$$

where $^{obs,bg}CO$ is the 20th percentile of the observed CO (Potosnak et al., 1999). When this leads to negative values of the CO offset, we assume a CO offset value of zero to avoid negative contributions to $^{ff}CO_2$. We then apply a revised static method to analyse the uncertainty due to non-anthropogenic influences as follows,

$$^{ff}CO_2 = (^{obs}CO - ^{obs.bg}CO - ^{chem}CO - ^{bb}CO)/20, \tag{5}$$

where ^{chem}CO is the net source of CO from the combined effects of OH oxidation sinks and VOC oxidation source, and ^{bb}CO is the biomass burning source component (described below).

The other two approaches are the model methods (Gerbig et al., 2003; Lin et al., 2004) which estimate the ratio R by transporting emission inventory fluxes with an atmospheric model. The model CO approaches can also be thought of as scaling the modelled fossil fuel CO_2 by the ratio of the observed to modelled fossil fuel CO. The basic model approach is formulated as

$$^{ff}CO_2 = (^{obs}CO - ^{mod.bg}CO)/\left(\frac{^{ff.mod}CO}{^{ff.mod}CO_2}\right), \tag{6}$$

where $^{ff,mod}CO_2$ and $^{ff,mod}CO$ are the concentrations resulting from driving the tracer model with fossil fuel inventories for CO_2 and CO, respectively, and $^{mod,bg}CO$ is the concentration resulting from driving the tracer model with only the boundary conditions (no emissions, no forest fire tracer). These model runs have no chemical reactions.

The revised model approach accounts for the non-anthropogenic CO influence as follows,

$$^{ff}CO_2 = (^{obs}CO - ^{mod.bg}CO - ^{chem}CO - ^{bb}CO)/\left(\frac{^{ff.mod}CO}{^{ff.mod}CO_2}\right). \tag{7}$$

Note that the model approaches (eqs. (6) and (7)) do not include any net chemistry effects on $^{ff,mod}CO$.

We will refer to the different methods in eqs. (4)–(7) as the static, revised static, model and revised model methods, respectively. We will compare these CO methods with the inventory method in which the $^{ff}CO_2$ is estimated by driving the atmospheric transport model with emissions inventories.

The overall chemistry concentrations are calculated as,

$$^{chem}CO = ^{mod}CO - ^{tracer}CO, \tag{8}$$

where ^{mod}CO is the full chemistry model result and $^{tracer}CO$ is the tracer model result (no chemistry). The chemistry values, ^{chem}CO, are the combination of the OH sink and the VOC source of CO,

$$^{chem}CO = ^{OH}CO + ^{VOC}CO, \tag{9}$$

where ^{VOC}CO is the VOC source of CO and ^{OH}CO is the OH sink of CO. The ^{VOC}CO source is estimated as the difference between the full chemistry model run and a full chemistry model run without VOC species in the emissions,

$$^{VOC}CO = ^{mod}CO - ^{novoc}CO, \tag{10}$$

where $^{novoc}CO$ is the CO prediction from a full chemistry CO model run with anthropogenic and biogenic VOC emissions removed from the surface flux. VOC species concentrations have been verified with ICARTT DC-8 and WP-3 measurements.

The biomass burning component is an important contributor to CO during the observation period. Significant forest fire emissions occurred outside of the model domain in Canada and Alaska. These forest fires are the largest on record for Alaska. In contrast to the observed data from Gerbig et al. (2003), the ICARTT data encountered collocated forest fire and fossil fuel CO. In order to use CO as a fossil fuel tracer, the biomass burning CO component must be estimated and subtracted from the CO observation.

Outside of forest fire plumes, we use the model runs driven by MOZART forest fire CO boundary conditions to provide a modelled biomass burning estimate, $^{mod,bb}CO$. For concentrated forest fire plumes (acetonitrile > 0.28 ppbv), the modelled forest fire CO greatly underestimates biomass burning CO. Therefore, the modelled forest fire CO is used when acetonitrile is less than 0.28 ppbv and a regression-based CO estimate is used when acetonitrile is greater than 0.28 ppbv,

$$^{bb}CO = ^{mod,bb}CO, \qquad \text{acetonitrile} < 0.28 \text{ ppbv}, \tag{11}$$

$$^{bb}CO = \alpha \cdot \text{acetonitrile} + \beta, \quad \text{acetonitrile} \geq 0.28 \text{ ppbv}, \tag{12}$$

where $^{mod,bb}CO$ is the modelled forest fire CO, α and β are the slope and intercept terms from the linear regression. The linear regression parameters are obtained by relating observed acetonitrile to estimated biomass burning CO, $^{obs,bb}CO$, where

$$^{obs,bb}CO = ^{obs}CO - (^{mod}CO - ^{mod,bb}CO). \tag{13}$$

We verified that the observed acetonitrile peaks are forest fire influenced and not anthropogenic by inspecting values of observed CH$_4$, NO$_2$ and SO$_2$.

During one interception of a power plant plume (LPS), we test SO$_2$ as an alternative tracer to CO. For LPS plumes, the CO approach may underestimate ^{ff}CO$_2$ when the true ratio of anthropogenic CO to CO$_2$ is less than the fixed ($R = 20$) or modelled ($R = {^{ff,mod}}$CO/^{ff,mod}CO$_2$) ratios. The SO$_2$ based ^{ff}CO$_2$ estimates are obtained by dividing observed SO$_2$ by the ratio of anthropogenic emissions of SO$_2$ to CO$_2$ for power plants within the influence region of the observation. The LPS emissions ratios are estimated with emissions data from the U.S. EPA's Clean Air Markets (EPA, 2006).

3. Results and discussion

3.1. Overview of observed and model results

Observations and model performance were analysed with a case study of the DC-8 flight during the day on 20 July 2004. This flight encountered a variety of important features for testing the CO method including urban pollution, LPS's, and regional forest fire plumes. In Fig. 1 the exaggerated altitude of the flight (height of bars) is shown along with the 3 min averaged ($\sim$30 km) CO$_2$ concentrations (colour of bars). The low-altitude segments of the flight pass over land cover that is primarily cropland in the Midwestern U.S. and forest in the Southeast. The low CO$_2$ concentrations near the surface result from the active summer biosphere in these regions.

Observation and model results from the 20 July flight are shown in the time-series in Fig. 2. In Fig. 2a, the CO$_2$ measurements are plotted along with the model results interpolated from the 60 km model domain. The model captures the general trend in CO$_2$ variation but misses the depth of the biosphere sink and the low-altitude CO$_2$ enhancements. The low-altitude CO$_2$ spikes consistently occur at the same times as elevated con-

centrations of observed anthropogenic tracers including CO in Fig. 2c and SO$_2$ in Fig. 2d. These low-altitude CO$_2$ enhancements are likely due to anthropogenic area sources and LPS's.

Figure 2b provides the time-series of the inventory driven fossil fuel CO$_2$ component along the flight path in comparison with the modelled ocean and biosphere contributions. The modelled fossil fuel CO$_2$ (inventory approach) is 1 to 5 ppm at low altitudes and is near zero in the free troposphere. From visual inspection of the observed CO$_2$ in Fig. 2a, the anthropogenic CO$_2$ spikes have approximate elevations of 4–10 ppm, with one very large plume of approximately 26 ppm at 17.1 hr.

The simultaneous peaks of CO and acetonitrile in Fig. 2c indicate very distinct forest fire plumes. The spikes of acetonitrile, the forest fire tracer, correspond with spikes in the CO concentrations at mid-altitudes near 17.4 hr and 21.6 hr. There are no corresponding spikes of SO$_2$ or other anthropogenic tracers that would indicate that this acetonitrile signal has an anthropogenic source. For other ICARTT flights, the mid-altitude band has an average CO level of 110 ppbv. For these mid-altitude forest fire plumes, the CO levels reach 362 and 370 ppbv, respectively. The forest fire source is likely to be from Alaskan or Canadian forest fires as indicated by the adjoint-derived influence region in Fig. 3.

The maximum model derived forest fire CO along the flight is 60 ppbv. The model results do not reflect the influence of the concentrated forest fire plumes because the forest fire influence is modelled in the boundary conditions using a global transport model with relatively coarse resolution.

3.2. CO method uncertainty

The oxidation of reduced carbon species to CO is a potential source of uncertainty for the CO method. During the summer, emissions of anthropogenic and biogenic VOC's result in significant secondary sources of CO. The model ^{voc}CO during the ICARTT period is typically low, with an average of 7 ppbv.
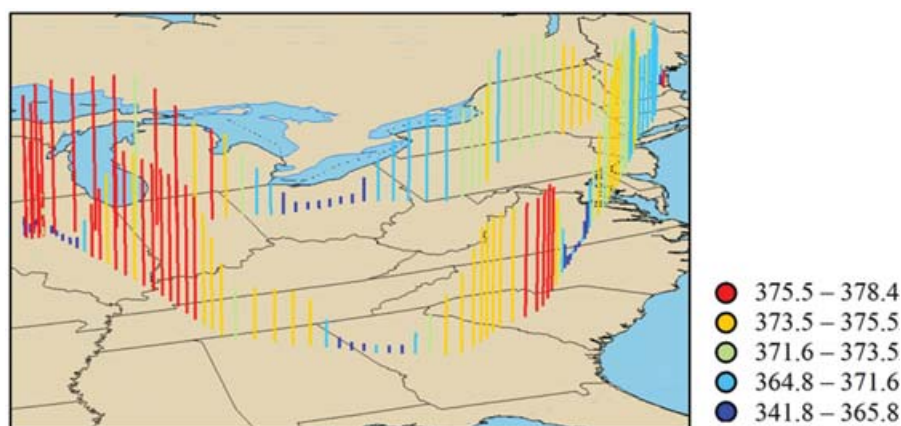

Fig. 1. NASA DC-8 flight on July 20, 2004. Heights of the bars are exaggerated altitude of flight path. Colour is observed CO$_2$ (ppm) with colour scheme by natural break (Jenks) method.
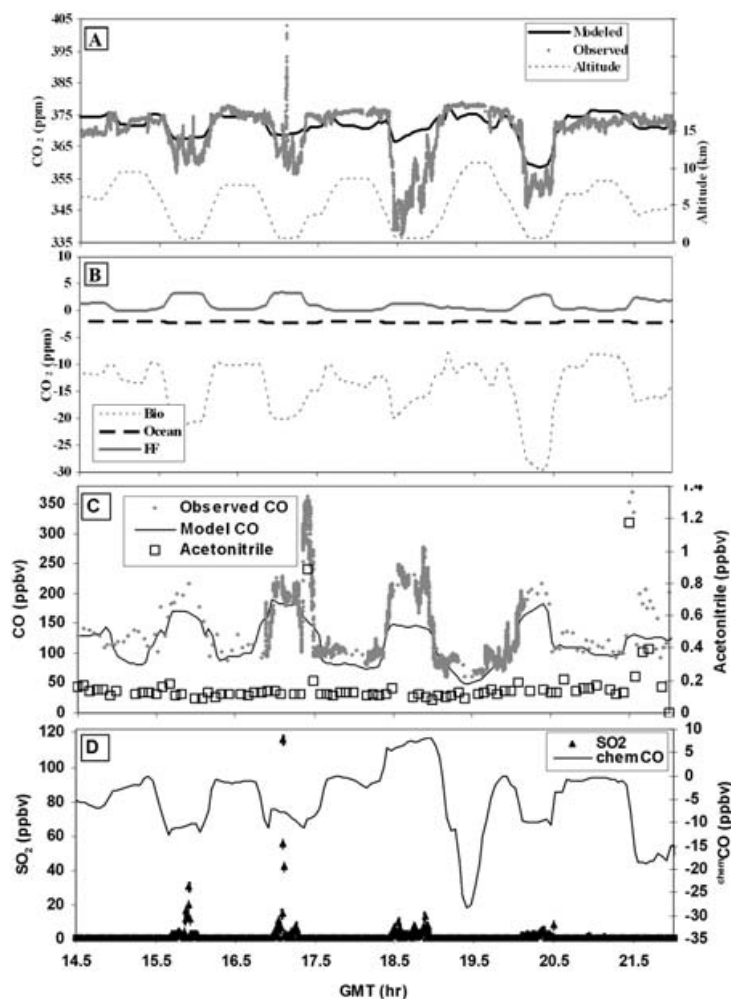
However, high values of ^{voc}CO as large as 85 ppbv occur at hot spots across the model domain, particularly over the southeast where biogenic emissions are high. In Fig. 4, a snapshot of the surface level ^{voc}CO on 20 July indicates up to 50 ppbv concentrations in the Midwest and the Southeast. A photochemical CO source of 50 ppbv results in an enhancement in $^{ff}CO_2$ of 2.5 ppm by the static CO method (eq. (4)).

The net CO production from chemical reactions, ^{chem}CO, is relatively small because the effect of the OH sink and VOC source tend to offset each other. The average ^{chem}CO value along the ICARTT flight paths is -5.3 ppbv indicating a slight net sink. However, there are hot spots across the model domain with net chemical sources in the southeast U.S. up to 83 ppbv and net chemical sinks in the Rocky Mountains as low as -75 ppbv. A net chemical CO concentration of 80 ppbv results in an adjustment in $^{ff}CO_2$ of 4 ppm by the static CO method. The net chemical contribution along the 20 July flight path is shown in Fig. 2d. The net chemical effect during this flight is primarily a sink, except near 18.5 hr where anthropogenic VOC emissions result in a net chemical source.

Forest fire sources are also a significant component of CO concentrations over North America. The effect of forest fires in Alaska and Canada during the ICARTT period on CO concentrations was estimated using model results and acetonitrile observations, a biomass burning tracer. In Fig. 5, the observed CO is plotted versus observed CO_2 along with colour coding for elevated acetonitrile. The general trend is a negative correlation of CO and CO_2 due to the co-location of the CO source and biogenic CO_2 sink at the surface. The forest fire influenced observations (circles) break from this trend with CO enhanced by up to 240 ppbv. A 240 ppbv increment in CO results in an increment of $^{ff}CO_2$ by the static CO method of 12 ppm.

The model estimates of forest fires CO result in an average contribution along all flight paths of 9.5 ppbv. The model estimates of ^{bb}CO along the ICARTT flight path greatly underestimate CO in the more concentrated plumes. In order to obtain a better estimate of biomass burning CO we apply observed and model results in a linear regression (see Section 2.3). We used elevated acetonitrile values greater than 0.28 ppbv to separate background acetonitrile from forest fire influenced acetonitrile.

Fig. 3. Three-day cone of influence for observation point on the July 20, 2004 flight path that intersected a forest fire plume (latitude 34°, longitude 274°, altitude 3.6 km). The values shown are normalized adjoint-derived sensitivities.
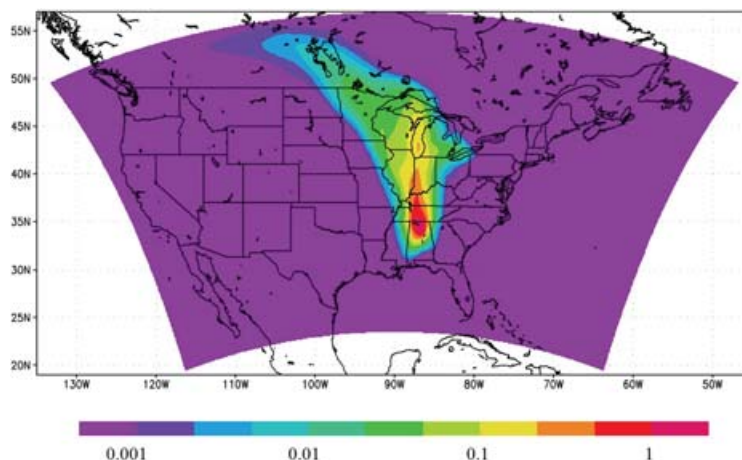

Fig. 4. Modelled CO mixing ratios from VOC oxidation (ppbv) at 21 hr (GMT), July 20th at surface model layer.
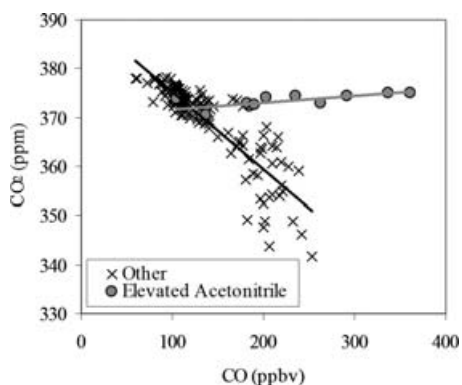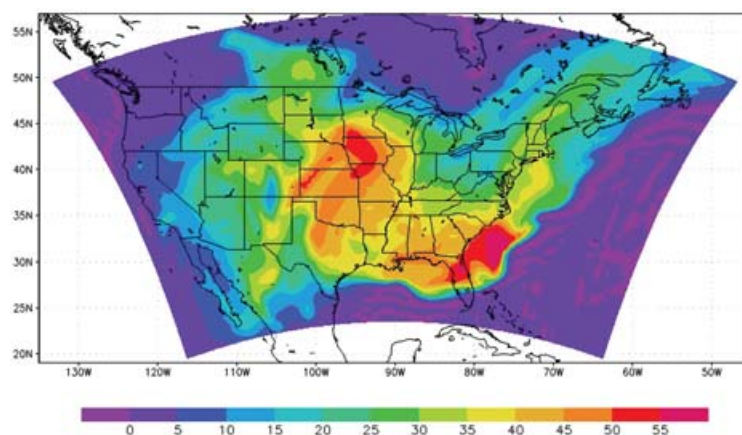

Fig. 5. Observed CO versus observed CO$_2$ along the July 20th ICARTT flight with colour coding for enhanced acetonitrile.

The linear regression has an R^2 of 0.92, indicating a strong relationship between the ^{bb}CO and acetonitrile in biomass burning plumes.

Preliminary comparison of model and measured CO$_2$ indicated that, in some cases, the ratio R was in error during interception of LPS plumes. We developed an alternative tracer (SO$_2$) method to provide a better ^{ff}CO$_2$ estimate, and calculate an alternative R in the LPS plume. One of the largest fossil fuel CO$_2$ plumes encountered in the ICARTT period occurs on 20 July at 17.1 hr (Fig. 2a). The CO peak at this time is not enhanced to the extent that the CO$_2$ peak is enhanced (Fig. 2c). However, the SO$_2$ measurements near this peak reflect the high intensity of the fossil fuel plume (Fig. 2d). The moderate enhancement of the CO collocated with the extreme enhancements of CO$_2$ and SO$_2$ are indicators of efficient LPS combustion.

The LPS emissions within the footprint of the observation are shown in Fig. 6. The observation point at 17.1 hr (marked X) is downstream of several large anthropogenic sources. The closest source in the influence region is the Wansley Electric Utility which burns coal and natural gas. The hourly emissions for Wansley indicate that the emitted ratio of SO$_2$ to CO$_2$ is significantly variable in time with a value of 0.0045 mol SO$_2$/mol CO$_2$ around the time of the large LPS observation.

In Fig. 7, the SO$_2$ and CO$_2$ observations in the plume are shown. The SO$_2$ observation point centred on the plume at 17.104 hr has a value of 116 ppbv. We make a rough estimate of the fossil fuel CO$_2$ in this plume as 26 ppm based on the difference between the average CO$_2$ values for the SO$_2$ sample period centred on
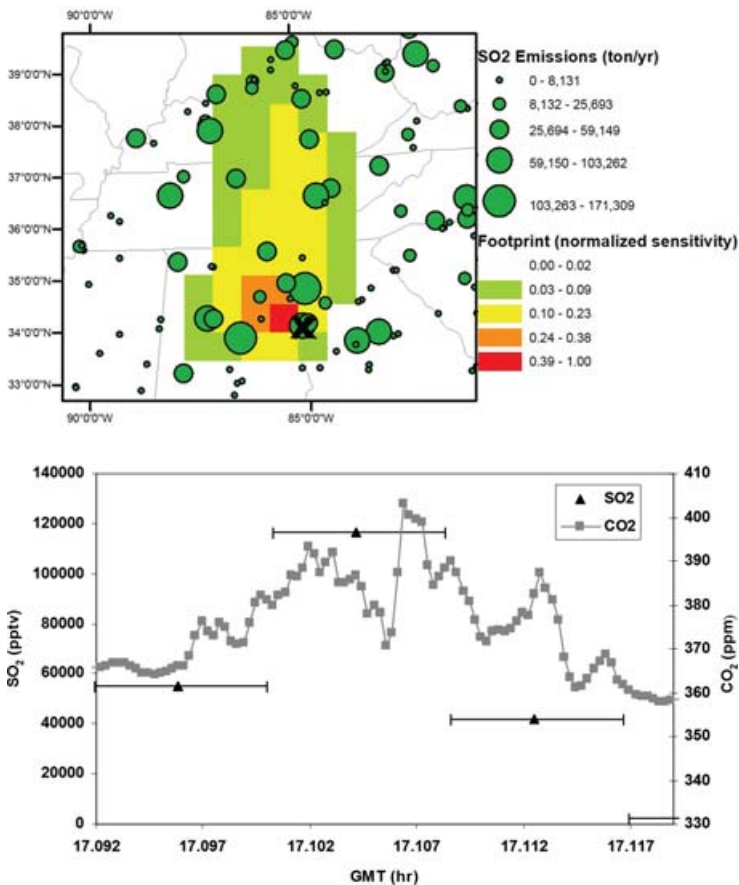
Fig. 6. Emissions sources for large anthropogenic spike observed during ICARTT at 17.1 hr GMT on July 20, 2004. The X marks the location of the observation. Shaded grid cells are the adjoint-derived footprint for the observation. Green circles are 2004 annual emissions of SO_2 from EPA Clean Sky Clean Air Markets inventory.
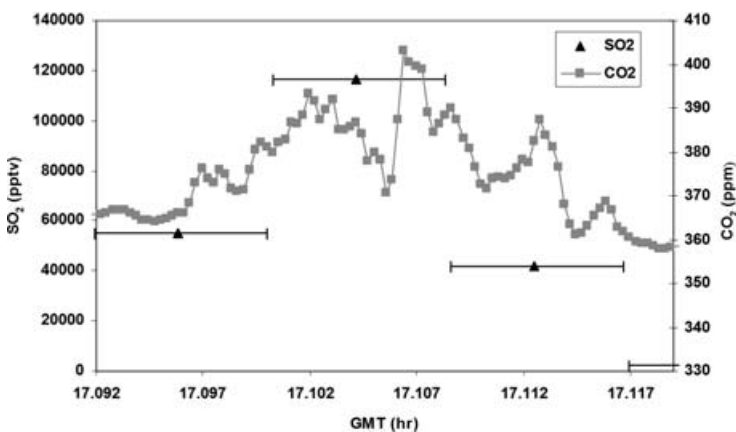
Fig. 7. Large anthropogenic spike of SO_2 and CO_2 around 17.1 hr on the July 20, 2004 ICARTT flight. Horizontal bars indicate sample intake period for SO_2.

17.104 and the average of the CO_2 values just before and after the plume. By dividing the observed SO_2 by the ratio of SO_2/CO_2 we estimate $^{ff}CO_2$ as 26 ppm. Back calculating the $CO:CO_2$ ratio R with the enhanced CO of 115 ppbv and estimated $^{ff}CO_2$ of 26 ppm gives an effective $CO:CO_2$ ratio $R' = 5$. Using the model CO method (eq. (6)) we estimate a much higher R value of 24.5. The difference between $^{ff}CO_2$ estimates for enhanced CO of 115 ppbv using the static R of 20 and revised R' of 5 is 20 ppm.

3.3. *Estimates of* $^{ff}CO_2$

By comparing the differences in $^{ff}CO_2$ calculated by the various methods, we can quantify the uncertainty related to several of the assumptions of the CO methods. Of all the possible comparisons that can be made, a few are most instructive. First, a comparison of the basic and revised CO methods (either using static R, or model-predicted R ratios) can inform us of the uncertainty expected due to the combined effect of the net chemical component and the forest fire component. Second, a comparison of the static methods (eqs. 4 and 5) versus the model methods (eqs. 6 and 7) quantifies the effect of assuming a spatially and temporally averaged R ratio versus one that reflects the spatial variation of the emission inventory.

For the 20 July flight, the revised static results are on average 0.8 ppm less than the static method results (Fig. 8a). The difference between the revised static and static methods is primarily due to forest fires and not the chemical component. The average forest fire CO source is 24 ppbv on this flight while the net chemical component is relatively small at −6 ppbv. However, near 19.5 hr the net chemical component is a strong sink (−28 ppbv) and the forest fire contribution is small, resulting in estimates of $^{ff}CO_2$ that are 1 ppm larger for the revised static method than the static method. Inside the forest fire plumes (near 17.4 hr and 21.5 hr), the static method is on average 8.2 ppm greater than the revised static method.

Estimates of $^{ff}CO_2$ based on the model CO approach and the revised model CO approach are shown in Fig. 8b. When the fossil fuel components are low, the modelled R ratio becomes very sensitive to errors in $^{mod,ff}CO$. To prevent unrealistic variability in R, we use the average model value of 23 when $^{mod,ff}CO$ is less than 4 ppbv. This accounts for 44% of values along the flight paths. The average difference between the revised model and model approach results is 0.7 ppm due to the forest fire contributions. Inside the forest fire plumes (near 17.4 hr and 21.5 hr), the static method is on average 7.2 ppm greater than the revised static method.

Fig. 8. Time series of ^{ff}CO$_2$ from inventory method (thin black line), CO methods that do not account for non-fossil fuel CO (grey line), and revised CO methods accounting for forest fires and photochemistry (thick black line). The static CO methods (eqs 4 and 5 with $R = 20$) are shown in A and the model CO methods (eqs 6 and 7 with estimated by the transport model) are shown in B.
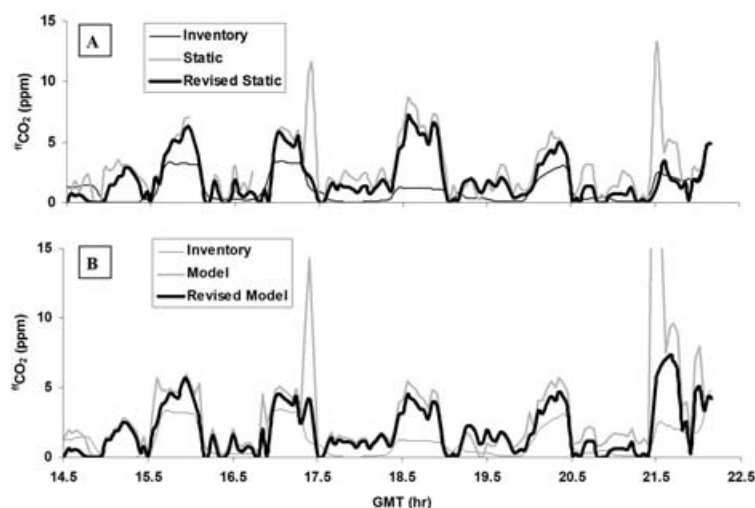

Fig. 9. Difference between ^{ff}CO$_2$ estimates from the revised model CO approach and the model CO approach (ppm CO$_2$) for all ICARTT DC8 flights.

For all flights, the revised methods tend to result in slightly lower values than the base case methods because the biomass burning CO is typically larger than the net chemical CO. The average difference in ^{ff}CO$_2$ between the model and revised model methods is 0.1 ppm. This difference is plotted for all flight paths in Fig. 9. Over half of the observation points have absolute differences of less than 0.5 ppm. The largest negative differences, ranging from -5 to -24 ppm, occur due to forest fire influences during the 20 July and 31 July flights. The most prominent positive differences, 1.4 to 2.6 ppm, occur offshore of the northeast and southeast where the VOC oxidation makes a large contribution to the CO concentration.

A comparison of the static methods (eqs. 4 and 5) with the model methods (eqs. 6 and 7) can be used to provide a preliminary estimate of the CO method uncertainty due to the assumption of a spatially uniform ratio R. For all ICARTT observations, the average difference between the revised model and the revised static approaches is 0.02 ppm due to the fact that the average model R value is similar to the static value. However, the dif-

ference between the revised model and model method estimates can be as high as 9.8 ppm in plumes where the model predicts efficient combustion ($R < 20$) and as small as -3.6 where the model predict inefficient combustion ($R > 20$).

For CO$_2$ inversion applications, the uncertainty in ^{ff}CO$_2$ propagates to the uncertainty in the residual concentrations, ^{r}CO$_2$, by eq. (1). For example, if unaccounted VOC sources resulted in an overestimate of ^{ff}CO$_2$ by the static CO method, then ^{r}CO$_2$ could be underestimated. The inversion model would then retrieve a decreased surface flux value which could be mistakenly interpreted as an increase in photosynthesis. To determine if the uncertainty in the CO method is significant relative to ^{r}CO$_2$, we estimate ^{r}CO$_2$ along the ICARTT flight path. The residual CO$_2$ is obtained by driving the transport model with the fluxes described in Section 2.1, including the inventory estimates of ^{ff}CO$_2$. The fraction of the CO uncertainty over the residual concentration is calculated to determine the significance of uncertainty for inversion applications. The average of the absolute value of this relative difference is 0.3 indicating that the uncertainty is significant relative to the residual concentration.

3.4. Comparison of CO method uncertainty with ^{14}CO$_2$ data

The CO method uncertainty estimates are compared with absolute error estimates from a study of ^{14}CO$_2$ by the NOAA GMD (Turnbull et al., 2006). Turnbull et al. (2006) measured boundary layer and background values for CO and ^{14}CO$_2$ on 2 August during an aircraft flight over a sampling site in the northeast (42° 57′ N, 72° 37′ W). Their results indicate that both the static CO method and the ^{14}CO$_2$ method yielded an ^{ff}CO$_2$ estimate of 4.2 ppm. Our model results also indicate that the static CO method should be accurate at this place and time. The model R value is 19 which is very similar to the static R value of 20. The modelled chemical sources and sinks are nearly balanced at the sampling time and location, with a ^{chem}CO value of -6 ppbv.

While the net chemical influence at this sampling site is small at the observation time, there are other times during August 2004 when the modelled net chemical sink is as extreme as -27 ppbv. There are also times during August at the sampling site when the static R value may be incorrect as indicated by model R values that range from 16 to 36. Unfortunately, the additional observations from Turnbull et al. (2006) are outside of the model simulation period. Future model runs that cover these other observations may be useful for interpreting the differences between CO and $^{14}CO_2$ method results as well as validating the revised CO method.

4. Summary

Analysis of uncertainty in the revised CO method leads to several conclusions related to estimating the fossil fuel component in observed CO_2:

1. If photochemical, biomass burning and LPS contributions are not considered, then these influences may incorporate uncertainty into CO-based $^{ff}CO_2$ by as much as 4, 12 and 24 ppm, respectively.

2. Combining acetonitrile and SO_2 observations with model results provides an alternative approach to estimating $^{ff}CO_2$ in concentrated biomass burning and LPS plumes.

3. The CO method uncertainty due to forest fire and photochemical influences is on average 30% of the residual CO_2 concentration along the ICARTT flight paths.

The analysis of model and observed tracers presented here, provided estimates of several aspects of uncertainty in the CO method due to non-anthropogenic components of the CO observation. Future studies of the CO method uncertainty should provide a more comprehensive analysis of errors in R. A complimentary approach to determining CO method uncertainty can be achieved with observations of CO and $^{14}CO_2$ that provide estimates of the absolute error in the CO method. For example, Turnbull et al. (2006) found underestimates of $^{ff}CO_2$ by the CO method of 1 to 5 ppm during winter and spring, with improved agreement during the summer. Combining the approach in the present study with the approach in Turnbull et al. (2006) would allow for the identification of the components of the absolute error, which could lead to improvements in the design of the CO method. Furthermore, the STEM-2K3 model could be used in forecast mode to identify observation times and locations in which uncertainty components such as the net chemical sinks would be most pronounced.

The revised CO method presented here was designed to extract the quantity of $^{ff}CO_2$ from an observation of CO while drawing on model and observed tracers to resolve uncertainties. The revised method could be further developed to incorporate SO_2 observations for reducing uncertainty due to LPS's. The usefulness of observed acetonitrile and SO_2 indicates that long term measurements of these species at carbon observatories would

be helpful for improving the CO method in future inversion studies.

5. Acknowledgments

Referencess

Andres, R. J., Marland, G., Fung, I. and Matthews, E. 1996. A 1 degrees x1 degrees distribution of carbon dioxide emissions from fossil fuel consumption and cement manufacture, 1950-1990. *Global Biogeochem. Cy.* **10**(3), 419–429.

Baker, I., Denning, A. S., Hanan, N., Prihodko, L., Uliasz, M. and co-authors 2003. Simulated and observed fluxes of sensible and latent heat and CO_2 at the WLEF-TV tower using SiB2.5. *Global Change Biol.* **9**(9), 1262–1277.

Bakwin, P., Davis, K., Yi, C., Wofsy, S., Munger, J. W. and co-authors 2004. Regional carbon dioxide fluxes from mixing ratio data. *Tellus* **56B**(4), 301–311.

Bakwin, P., Tans, P. P., White, J. W. C. and Andres, R. J. 1998. Determination of the isotopic ($^{13}C/^{12}C$) discrimination by terrestrial biology from a global network of observations. *Global Biogeochem. Cy.* **12**(3), 555–562.

Barletta, B., Meinardi, S., Simpson, I. J., Khwaja, H. A., Blake, D. R. and co-authors 2002. Mixing ratios of volatile organic compounds (VOCs) in the atmosphere of Karachi, Pakistan. *Atmos. Environ.* **36**(N21), 3429–3443.

Blasing, T. J., Broniak, C. and Marland, G. 2004. Estimates of monthly carbon dioxide emissions and associated $\delta^{13}C$ values from fossil-fuel consumption in the U.S.A. In: Trends: A Compendium of Data on Global Change, Carbon Dioxide Information Analysis Center, Oak Ridge National Laboratory, U.S. Department of Energy, Oak Ridge, Tennessee.

Blasing, T. J., Broniak, C. T. and Marland, G. 2003. Preliminary estimates of the annual cycle of fossil fuel emissions from the USA. In: Carbon Dioxide Inf. Anal. Cent., Oak Ridge Natl. Lab., Oak Ridge, Tennessee.

Bousquet, P., Peylin, P., Ciais, P., Le Quere, C., Friedlingstein, P. and co-authors 2000. Regional changes in carbon dioxide fluxes of land and oceans since 1980. *Science* **290**(5495), 1342–1346.

Brenkert, A. L. 1998. Carbon dioxide emission estimates from fossil-fuel burning, hydraulic cement production, and gas flaring for 1995 on a one degree grid cell basis. http://cdiac.esd.ornl.gov/epubs/ndp/ndp058a/ndp058a.html

Carmichael, G. R., Tang, Y., Kurata, G., Uno, I., Streets, D. and co-authors 2003. Regional-scale chemical transport modeling in support of the analysis of observations obtained during the TRACE-P experiment. *J. Geophys. Res.* **108**(D21), 8823, doi:8810.1029/2002JD003100.

Carter, W. 2000. Documentation of the SAPRC-99 chemical mechanism for VOC reactivity assessment, Final Report to California Air

Resources Board Contract No. 92-329. University of California, Riverside, California.

Chai, T. F., Carmichael, G. R., Sandu, A., Tang, Y. H. and Daescu, D. N. 2006. Chemical data assimilation of transport and chemical evolution over the Pacific (TRACE-P) aircraft measurements. *J. Geophys. Res.* **111**(D02301), doi:10.1029/2005JD005883.

Daescu, D. N. and Carmichael, G. R. 2003. An adjoint sensitivity method for the adaptive location of the observations in air quality modeling. *J. Atmos. Sci.* **60**(2), 434–449.

Enting, I. G., Trudinger, C. M. and Francey, R. J. 1995. A synthesis inversion of the concentration and del^{13}C of atmospheric CO$_2$. *Tellus* **47B**(1-2), 35–52.

EPA 2006. US EPA Clean Air Market Database, Available at: http://www.epa.gov/airmarkt/.

Fan, S., Gloor, M., Mahlman, J., Pacala, S., Sarmiento, J. and co-authors 1998. A large terrestrial carbon sink in North America implied by atmospheric and oceanic carbon dioxide data and models. *Science* **282**(5388), 442–446.

Gerbig, C., Lin, J. C., Wofsy, S. C., Daube, B. C., Andrews, A. E. and co-authors 2003. Toward constraining regional-scale fluxes of CO$_2$ with atmospheric observations over a continent: 2. Analysis of COBRA data using a receptor-oriented framework. *J. Geophys. Res.* **108**(D24), 4757, doi:4710.1029/2003JD003770.

Geron, C. D., Guenther, A. B. and Pierce, T. E. 1994. An improved model for estimating emissions of volatile organic-compounds from forests in the eastern united-states. *J. Geophys. Res.* **99**(D6), 12773–12791.

Grell, G. A., Dudhia, J. and Stauffer, D. R. 1994. A description of the fifth-generation Penn State/NCAR Mesoscale Model (MM5). NCAR Technical Note, NCAR/TN-398+STR, Boulder, Colorado.

Gurney, K. R., Law, R. M., Denning, A. S., Rayner, P. J., Baker, D. and co-authors 2002. Towards robust regional estimates of CO$_2$ sources and sinks using atmospheric transport models. *Nature* **415**(6872), 626–630.

Gurney, K. R., Law, R. M., Denning, A. S., Rayner, P. J., Baker, D., and co-authors 2003. TransCom 3 CO$_2$ inversion intercomparison: 1. Annual mean control results and sensitivity to transport and prior flux information. *Tellus* **55B**(2), 555–579.

Gurney, K. R., Law, R. M., Denning, A. S., Rayner, P. J., Pak, B. C. and co-authors 2004. Transcom 3 inversion intercomparison: Model mean results for the estimation of seasonal carbon sources and sinks. *Global Biogeochem. Cy.* **18**(GB1010), doi:10.1029/2003GB002111.

Gurney, K. R., Yu-Han, C., Maki, T., Kawa, S. R., Andrews, A. E. and co-authors 2005. Sensitivity of atmospheric CO$_2$ inversions to seasonal and interannual variations in fossil fuel emissions. *J. Geophys. Res.* **110**(D10308), doi:10.1029/2004JD005373.

Hakami, A., Henze, D. K., Seinfeld, J. H., Chai, T., Tang, Y. and co-authors 2005. Adjoint inverse modeling of black carbon during the Asian Pacific Regional Aerosol Characterization Experiment. *J. Geophys. Res.* **110**(D14301), doi:10.1029/2004JD005671.

Hong, S.-Y. and Pan, H.-L. 1996. Nonlocal boundary layer vertical diffusion in a medium-range forecast model. *Mon. Weather Rev.* **124**(10), 2322–2339.

Huey, L. G., Tanner, D. J., Slusher, D. L., Dibb, J. E., Arimoto, R. and co-authors 2004. CIMS measurements of HNO$_3$ and SO$_2$ at the South Pole during ISCAT 2000. *Atmos. Environ.* **38**(32), 5411–5421.

Law, R. M., Peters, W. and Rodenbeck, C. 2005. Protocol for TransCom continuous data experiment, TransCom Aspendale, Victoria, Australia.

Levin, I., Kromer, B., Schmidt, M. and Sartorius, H. 2003. A novel approach for independent budgeting of fossil fuel CO$_2$ over Europe by ^{14}CO$_2$ observations. *Geophys. Res. Lett.* **30**(23), 2194.

Levin, I., Schuchard, J., Kromer, B. and Munnich, K. O. 1989. The Continental European Suess Effect. *Radiocarbon* **31**(3), 431–440.

Lin, J. C., Gerbig, C., Wofsy, S. C., Andrews, A. E., Daube, B. C. and co-authors 2004. Measuring fluxes of trace gases at regional scales by Lagrangian observations: Application to the CO$_2$ Budget and Rectification Airborne (COBRA) study. *J. Geophys. Res.* **109**(D15304), doi:10.1029/2004JD004754.

Lobert, J. M., Scharffe, D. H., Kuhlbusch, T. A., Seuwen, R. and Crutzen, P. J. 1991. Experimental evaluation of biomass burning emissions: Nitrogen and carbon containing compounds. In: *Global Biomass Burning: Atmospheric, Climatic, and Biospheric Implications* (ed. J. S. Levine). MIT Press, Cambridge, Massachusetts, 289–304.

Olivier, J. G., Bouwman, J., Van der, A. F. Maas, C. W. M., Berdowski, J. J. M. and co-authors 1996. Description of EDGAR Version 2.0. A set of global emission inventories of greenhouse gases and ozone-depleting substances for all anthropogenic and most natural sources on a per country basis and on 1 x 1 grid. In: Natl. Inst. for Public Health and the Environ., Bilthoven, The Netherlands.

Peters, W., Krol, M. C., Dlugokencky, E. J., Dentener, F. J., Bergamaschi, P. and co-authors 2004. Toward regional-scale modeling using the two-way nested global model TM5: Characterization of transport using SF6. *J. Geophys. Res.* **109**(D19314), doi:10.1029/2004JD005020.

Pfister, G., Hess, P. G., Emmons, L. K., Lamarque, J.-F., Wiedinmyer, C. and co-authors 2005. Quantifying CO emissions from the 2004 Alaskan wildfires using MOPITT CO data. *J. Geophys. Res.* **32**(L11809), doi:10.1029/2005GL022995.

Potosnak, M. J., Wofsy, S. C., Denning, S. A., Conway, T. J., Munger, J. W. and co-authors 1999. Influence of biotic exchange and combustion sources on atmospheric CO$_2$ concentrations in New England from observations at a forest flux tower. *J. Geophys. Res.* **104**(D8), 9561–9569.

Sachse, G. W., Hill, G. F., Wade, L. O. and Perry, M. G. 1987. Fast-response, high-precision carbon-monoxide sensor using a tunable diode-laser absorption technique. *J. Geophys. Res.* **92**(D2), 2071–2081.

Sandu, A., Daescu, D. N., Carmichael, G. R. and Chai, T. 2005. Adjoint sensitivity analysis of regional air quality models. *J. Comp. Phys.* **204**(1), 222–252.

Singh, H. B., Salas, L., Herlth, D., Kolyer, R., Czech, E. and co-authors 2003. In situ measurements of HCN and CH$_3$CN over the Pacific Ocean: Sources, sinks, and budgets. *J. Geophys. Res.* **108**(D20), 8795, doi:8710.1029/2002JD003006.

Takahashi, T., Wanninkhof, R. H., Feely, R. A., Weiss, R. F., Chipman, D. W. and co-authors 1999. Net sea-air CO$_2$ flux over the global oceans: An improved estimate based on the sea–air pCO$_2$ difference. In: 2nd *CO$_2$ in Oceans Symposium* Cent. for Global Environ. Res. Natl. Inst. for Environ. Stud., Tsukuba, Japan.

Tang, Y. H., Carmichael, G. R., Horowitz, L. W., Uno, I., Woo, J. H. and co-authors 2003. Impacts of aerosols and clouds on photolysis frequencies and photochemistry during TRACE-P: 2. Three dimensional study using a regional chemical transport model. *J. Geophys. Res.* **108**(D21), 8822.

Tang, Y. H., Carmichael, G. R., Seinfeld, J. H., Dabdub, D., Weber, R. J. and co-authors 2004. Three-dimensional simulations of inorganic aerosol distributions in east Asia during spring 2001. *J. Geophys. Res.* **109**(D19S23), doi:10.1029/2004JD005373.

Tans, P. P., Fung, I. Y. and Takahashi, T. 1990. Observational constraints on the global atmospheric CO_2 budget. *Science* **247**(4949), 1431–1439.

Turnbull, J. C., Miller, J. B., Lehman, S. J., Tans, P. P., Sparks, R. J. and co-authors 2006. Comparison of $^{14}CO_2$, CO, and SF_6 as tracers for recently added fossil fuel CO_2 in the atmosphere and implications for biological CO_2 exchange. *Geophys. Res. Lett.* **33**(L01817), doi:10.1029/2005GL024213.

Vay, S. A., Woo, J.-H., Anderson, B. E., Thornhill, K. L., Blake, D. R. and co-authors 2003. Influence of regional-scale anthropogenic emissions on CO_2 distributions over the western North Pacific. *J. Geophys. Res.* **108**(D20), 8801, doi:8810.1029/2002JD003094.

Wofsy, S. S. and Harris, R. C. 2002. North American Carbon Plan (NACP). Report of the NACP Committee of the U.S. Interagency Carbon Cycle Science Program. In: US Global Change Research Program, Washington, DC.

Zondervan, A. and Meijer, J. A. J. 1996. Isotopic characterisation of CO_2 sources during regional pollution events using isotopic and radiocarbon analysis. *Tellus* **48B**(4), 601–612.